Push-Pull Intermolecular Nucleophile–Electrophile Interactions of Carbonyl Groups from Crystallographic Data and MNDO Calculations

Michèle Cossu,[1a] Christian Bachmann,[1a] Thomas Yao N'Guessan,[1a] Robert Viani,[1a,d] Jacques Lapasset,[1b] Jean-Pierre Aycard,[1c] and Hubert Bodot*[1c]

Départements de Physique et de Chimie, Faculté des Sciences et Techniques, Université Nationale de Côte d'Ivoire, Abidjan 04, Côte d'Ivoire, Laboratoire de Minéralogie et Cristallographie, UA CNRS 233, Université des Sciences et Techniques du Languedoc, 34060 Montpellier Cedex, France, and Département de Physique des Interactions Ioniques et Moléculaires, Equipe de Spectrométrie Appliquée, UA CNRS 773, Université de Provence, 13398 Marseille Cedex 13, France

Received April 21, 1987

From the crystallographic data of 18 achiral mono- and polycyclic anhydrides of C_s and C_{2v} symmetry, the environment around each carbonyl group was investigated in order to characterize the different nucleophile–electrophile (Nu–El) intermolecular interactions O···C=O and C=O···H ("acidic" hydrogen). For O···C=O interactions, typical geometrical features are observed. The carbonyl groups are often involved in push–pull interactions such as C=O···C=O···C=O, especially for the nine achiral anhydrides that crystallize in the $P_{2_12_12_1}$ chiral space group. The conformation of the anhydride ring is envelope (6 molecules) or half-chair (12 molecules); in the latter case, the molecules turn into chiral species. MNDO calculations have been performed to model the intermolecular interactions. In contrast to the nucleophilic approach, which is very dependent on geometry and consequently on steric hindrance control, the electrophilic approach is efficient whatever its orientation and therefore is quite independent of steric factors. Pyramidalizations on the carbonyl group occur for Nu···C=O and C=O···El interactions, with the substrate carbon atom moving in the half-space where the reactant is located. Additive pyramidalizations are observed when push–pull interactions are efficient; therefore, weak pyramidalizations do not mean weak interactions when the nucleophile and the electrophile are in opposite half-spaces. Other MNDO calculations show that the anhydride ring is easily puckered to a half-chair conformation; it is more difficult to get the envelope form, but in every case, these processes induce spontaneous pyramidalizations, as is experimentally observed with some carbonyl groups not involved in O···C=O interactions.

The analysis of crystallographic data has recently improved our structural knowledge about reaction paths of heterolytic reactions,[2] especially for nucleophilic addition to carbonyl groups.[3] Intramolecular[3a] and intermolecular[3b] donor–acceptor interactions have been analyzed in terms of geometrical parameters: distance d(Nu···C=O) between the reactant nucleophilic atom and the electrophilic carbon of the carbonyl group, angle θ(Nu···C=O) always close to 105°, pyramid height Δ between the top carbonyl carbon and the base consisting of the oxygen and the two other atoms covalently bonded to the carbonyl carbon. Moreover, the Nu atom is always very close to the carbonyl bisector plane, another typical geometrical feature of these interactions.

For Nu = N, an almost perfect correlation associates Δ and d; as has been established from intermolecular interaction data of cyclic molecules,[3a] it allows the investigation of a broad range of d values up to covalent distances.

For Nu = O, intra- and intermolecular interactions have been investigated,[3b] but Δ values are less than those observed for Nu = N at similar d values. A premature conclusion might be that these O···C=O interactions are too weak to be significant. But our careful investigation of the molecular packings in a series of 18 cyclic anhydrides[4]

Chart I[a]

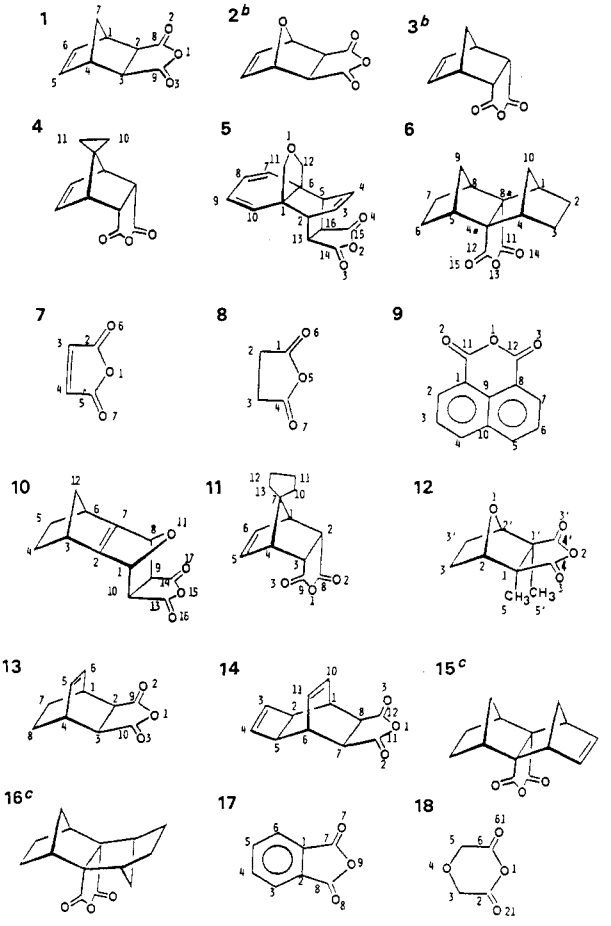

[a] Numberings as in the original publications. [b] Numbering as that of 1. [c] Numbering as that of 6.

(1) (a) Université Nationale de Côte d'Ivoire. (b) USTL, Montpellier. (c) Université de Provence. (d) Present address: Laboratoire de Biophysique, Université de Nice, 06034 Nice Cedex, France.

(2) Bürgi, H. B.; Dunitz, J. D. *Acc. Chem. Res.* **1983**, *16*, 153–161.

(3) (a) Bürgi, H. B.; Dunitz, J. D.; Shefter, E. *J. Am. Chem. Soc.* **1973**, *95*, 5065–5067. (b) Bürgi, H. B.; Dunitz, J. D.; Shefter, E. *Acta Crystallogr., Sect. B: Struct. Crystallogr. Cryst. Chem.* **1974**, *B30*, 1517–1527. (c) Bürgi, H. B.; Lehn, J. M.; Wipff, G. *J. Am. Chem. Soc.* **1974**, *96*, 1956–1957. (d) Bürgi, H. B.; Dunitz, J. D.; Lehn, J. M.; Wipff, G. *Tetrahedron* **1974**, *30*, 1563–1572. (e) Richard, E.; Rosenfield, J.; Dunitz, J. D. *Helv. Chim. Acta* **1978**, *61*, 2176–2189. (f) Schweitzer, W. B.; Procter, G.; Kaftory, M.; Dunitz, J. D. *Ibid.* **1978**, *61*, 2783–2802. (g) Procter, G.; Britton, D.; Dunitz, J. D. *Ibid.* **1981**, *64*, 471–477. (h) Kayser, M.; Eisenstein, O. *Can. J. Chem.* **1981**, *59*, 2457–2462. (i) Chadwick, D. J.; Whittleton, S. N.; Small, R. W. H. *J. Chem. Soc., Perkin Trans. 2* **1982**, 669–676. (j) Chadwick, D. J.; Whittleton, S. N. *J. Chem. Res., Synop.* **1984**, 398–399; *J. Chem. Res., Miniprint* **1984**, 3764–3785. (k) Murray-Rust, P.; Gluster, J. P. *J. Am. Chem. Soc.* **1984**, *106*, 1018–1025. (l) Jeffrey, G. A.; Houk, K. N.; Paddon-Row, M. N.; Rondan, N. G.; Mitra, J. *J. Am. Chem. Soc.* **1985**, *107*, 321–326.

0022-3263/87/1952-5313$01.50/0

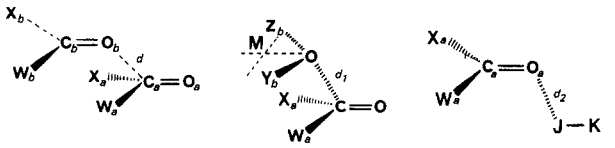

1.1 1.2 1.3

parameters	1.1	1.2	1.3
θ_1	$C_bO_bC_a$	MO_bC_a	C_aO_aJ
θ_2	$O_bC_aO_a$	$O_bC_aO_a$	O_aJK
Φ_1	$W_bC_bO_bC_a$	$Y_bZ_bO_bC_a$	$W_aC_aO_aJ$
Φ_2	$C_bO_bC_aO_a$	$MO_bC_aO_a$	C_aO_aJK
Φ_3	$O_bC_aO_aW_a$	$O_bC_aO_aW_a$	

Types of molecules and bonds: anhydrides, W = C, X = O–CO–, Y = Z = CO–; ethers, Y = Z = C; formaldehyde, W = X = H; water, Y = Z = H; J–K = H–C; C–O (ether); H–F; Li–H.

Figure 1. Geometrical parameters for the intermolecular interactions. (1.1) Substrate–reactant: a–b ($d = d_1$); b–a ($d = d_2$). (1.2) O···M bisector of $Y_bO_bZ_b$.

(Chart I) having C_s or C_{2v} symmetry draws our analysis to another conclusion. In this series, many C=O···C=O intermolecular interactions and some >O···C=O interaction may be suspected as they are in agreement with two of the geometrical criteria: $\theta \simeq 105°$ and bisector nucleophile attack. To justify the weakness of the corresponding pyramidalizations (Δ values), one may postulate perturbations from supplementary nucleophile–electrophile interactions, either secondary counteracting Nu···C=O[3b] or C=O···El interactions, with the electrophilic (El) atom being carbonyl carbon or hydrogen atoms of neighboring molecules. The role played by C–H···O interactions in determining molecular packing has been recently emphasized.[5] Moreover, each anhydride of our series, except

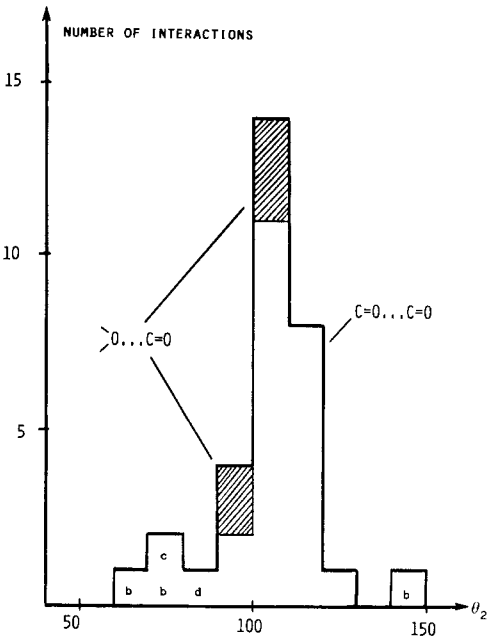

Figure 2. Distribution of O···C=O angles θ_2 (from Tables VIII and IX) from crystallographic data[4] of the anhydride series. Key: (b) secondary O···C=O interaction weaker than the primary one, which has the shortest O···C distance (4 and 18); (c) head-to-tail orientation of the two interacting carbonyl groups, $\Phi_2 = 0°$ (14); (d) weak interaction, $d_1 = 3.56$ Å (5).

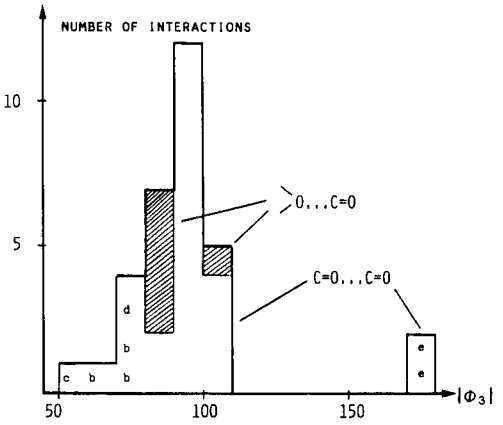

Figure 3. Distribution of $|\Phi_3|$ dihedral angles (Figure 1; values from Tables VIII and IX) from crystallographic data[4] of the anhydride series. Key: (b–d) details in Figure 2; (e) interactions in 18 crystal.

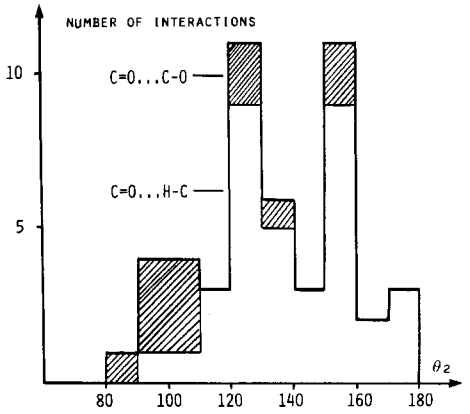

Figure 4. Distribution of O···J–K angles θ_2 (values from Tables X and XI) from crystallographic data[4] of the anhydride series. See Figure 1, 1.3; J–K = H–C and C–O.

6 and 16, provides hydrogen atoms as weak electrophiles owing to their bonding to C(sp^2), C(sp^3)–O, and/or C-

(4) (a) 1, bicyclo[2.2.1]hept-5-ene-2,3-*exo*-dicarboxylic anhydride: Filippini, G.; Gramaccioli, C. M.; Rovere, C.; Simonetta, M. *Acta Crystallogr. Sect. B: Struct. Crystallogr. Cryst. Chem.* **1972**, *B28*, 2869–2874. (b) 2, 7-oxabicyclo[2.2.1]hept-5-ene-2,3-*exo*-dicarboxylic anhydride: Baggio, S.; Barriola, A.; de Perazzo, P. K. *J. Chem. Soc. Perkin Trans. 2* **1972**, 934–938. (c) 3, bicyclo[2.2.1]hept-5-ene-2,3-*endo*-dicarboxylic anhydride: Destro, R.; Filippini, G.; Gramaccioli, C. M.; Simonetta, M. *Acta Crystallogr., Sect. B: Struct. Crystallogr. Cryst. Chem.* **1969**, *B25*, 2465–2472. (d) 4, 7-spirocyclopropylbicyclo[2.2.1]hept-5-ene-2,3-*endo*-dicarboxylic anhydride: Craig, R. E. R.; Craig, A. C.; Larsen, R. D.; Caughlan, C. N. *J. Org. Chem.* **1976**, *41*, 2129–2133. (e) 5, monoadduct between 12-oxo[4.4.3]propella-2,4,7,9-tetraene and maleic anhydride: Kaftory, M. *Acta Crystallogr., Sect. B: Crystallogr. Cryst. Chem.* **1980**, *B36*, 597–606. (f) 6, 1,2,3,4,4a,5,6,7,8,8a-decahydro-1,4,5,8-*exo,exo*-dimethanonaphthalene-4a,8a-dicarboxylic anhydride: Bartlett, P. D.; Blakeney, A. J.; Kinura, M.; Watson, W. H. *J. Am. Chem. Soc.* **1980**, *102*, 1383–1390. (g) 7, maleic anhydride: Marsh, R. E.; Ubell, E.; Wilcox, H. E. *Acta Crystallogr.* **1962**, *15*, 35–41. (h) 8, succinic anhydride: Ehrenberg, M. *Acta Crystallogr.* **1965**, *19*, 698–703. (i) 9, naphthalene-1,8-dicarboxylic anhydride: Grigoreva, L. P.; Chetkina, L. A. *Sov. Phys. Crystallogr. (Engl. Trans.)* **1975**, *20*, 1289–1291. (j) 10, 11-oxa-*endo*-tetracyclo[6.2.1.1^{3,6}.0^{2,7}]dodec-2(7)-ene-9,10-*exo*-dicarboxylic anhydride: Hagenbuch, J. P.; Vogel, P.; Pinkerton, A. A.; Schwarzenbach, D. *Helv. Chim. Acta* **1981**, *64*, 1818–1832. (k) 11, 7-spirocyclopentylbicyclo-[2.2.1]hept-5-ene-2,3-*endo*-dicarboxylic anhydride: Craig, R. E. R.; Craig, A. C.; Larsen, R. D.; Caughlan, C. N. *J. Org. Chem.* **1977**, *42*, 3188–3190. (l) 12, 2,3-dimethyl-7-oxabicyclo[2.2.1]heptane-2,3-*exo*-dicarboxylic anhydride: Zehnder, M.; Thewalt, U. *Helv. Chim. Acta* **1977**, *60*, 740–742. (m) 13, bicyclo[2.2.2]oct-5-ene-2,3-*endo*-dicarboxylic anhydride: Destro, R.; Filippini, G.; Gramaccioli, C. M.; Simonetta, M. *Acta Crystallogr., Sect. B: Struct. Crystallogr. Cryst. Chem.* **1971**, *B27*, 2023–2028. (n) 14, *anti*-tricyclo[4.2.2.0^{2,5}]deca-3,9-diene-7,8-*endo*-dicarboxylic anhydride: Filippini, G.; Induni, G.; Simonetta, M. *Ibid.* **1973**, *B29*, 2471–2476. (o) 15, 1,2,3,4,4a,5,8,8a-octahydro-1,4,5,8-*exo,exo*-dimethanonaphthalene-4a,8a-dicarboxylic anhydride: Reference 4f. (p) 16, 1,2,3,4,4a,5,6,7,8,8a-decahydro-1,4,5,8-*exo,endo*-dimethanonaphthalene-4a,8a-dicarboxylic anhydride: Reference 4f. (q) 17, phthalic anhydride: Bates, R. B.; Cutler, R. S. *Acta Crystallogr., Sect. B: Struct. Crystallogr. Cryst. Chem.* **1977**, *B33*, 893–895. (r) 18, 1,4-dioxacyclohexane-2,6-dione: Brisse, F.; Sygusch, J. *Ibid.* **1975**, *B31*, 2829–2832.

(5) (a) Taylor, R.; Kennard, O. *J. Am. Chem. Soc.* **1982**, *104*, 5063–5070. (b) Berkovitch-Yellin, Z.; Leiserowitz, L. *Acta Crystallogr., Sect. B: Struct. Sci.* **1984**, *B40*, 159–165. (c) Taylor, R.; Kennard, O. *Acc. Chem. Res.* **1984**, *17*, 320–326. (d) Sarma, J. A. R. P.; Desiraju, G. R. *Ibid.* **1986**, *19*, 222–228.

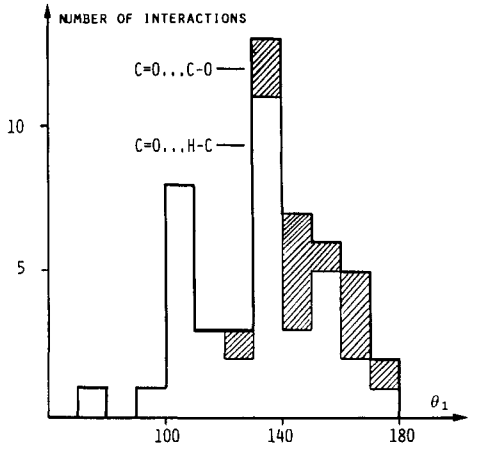

Figure 5. Distribution of C=O···J angles θ_1 (values from Tables X and XI) from crystallographic data[4] of the anhydride series. See Figure 1, 1.3; J–K = H–C and C–O.

(sp^3)–$C(sp^2)$ (–C(=O)–O or –C=C–).

To check the efficiency of these postulated Nu···C=O···El push–pull interactions, their experimental geometrical features have been compared with those resulting from MNDO calculations using the H_2C=O and HC(O)-OC(O)H systems, associated with different neighboring nucleophile and/or electrophile, as models.

Experimental Geometrical Features

From the crystal data of 18 C_s or C_{2v} monocyclic or polycyclic anhydrides[4,6] without any heteroatom except oxygen, we have calculated the different geometrical parameters associated with the suspected intermolecular nucleophile–electrophile interactions. These have been selected on the basis of intermolecular atomic distances in general shorter than the sum of Allinger's van der Waals radii,[7a] well established through MM2 molecular mechanics modeling, which takes into account in particular the revised hydrogen van der Waals radii (1.4 Å).[7b]

The geometrical parameters are defined in Figure 1, reported in Tables VIII–XI in the supplementary material, and analyzed as distribution diagrams in Figures 2–5.

Oxygen–Carbon Intermolecular Interactions. Anhydrides **1–5**, **7–9**, **12**, **14**, **17**, and **18** are involved in different kinds of interactions: 26 C=O···C=O (intermolecular O···C distances d ranging from 2.90 to 3.58 Å); 6 >O···C=O (3.05 ≤ d ≤ 3.59 Å); 12 C=O···C–O (3.20 ≤ d ≤ 3.44 Å).

The distributions of the θ_2 and Φ_3 values for the 32 O···C=O interactions are shown in Figures 2 and 3, respectively. The averaged values of θ_2 and Φ_3 are 104° and 95°, respectively, in good agreement with Bürgi's results.[3a,c] Only four θ_2 values are less than 90° and correspond to Φ_3 values clearly out of the bisector criteria ($\Phi_3 \sim 90°$), but the corresponding O···C distances (3.31–3.58 Å) are rather large. In two other cases, the nucleophilic oxygen is almost in the plane of the carbonyl group ($|\Phi_3|$ = 172–173°), but it corresponds to anhydride **18** involved in numerous O···C=O interactions.

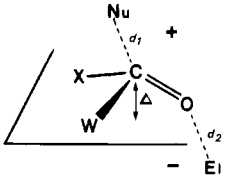

Figure 6. Carbonyl group pyramidalization.

If we exclude these 6 uncertain interactions, we register the carbonyl groups to be involved in push–pull interactions: 11 C=O···C=O···C=O; 2 >O···C=O···C=O, 3 C=O···C=O···C–O, and 4 >O···C=O···C–O.

Focusing on the C=O reactant orientation, the Φ_1 angles appear quite homogeneously distributed from 4 to 174° (Table VIII, supplementary material).

Carbonyl Oxygen–Hydrogen Intermolecular Interactions. From the 47 hydrogen atoms selected by the intermolecular distance criteria (O···H ≤ 2.75 Å), only 9 do not have electrophilic character as defined in the introduction; they will be excluded from the registration of C=O···H intermolecular interactions (Table X, supplementary material).

As the hydrogen positions are not accurately known, the errors on O···H distances may be larger than 0.1 Å. Therefore, the fluctuations of d values cannot be significant. The distribution diagrams of θ_2 and θ_1 geometrical parameters (Figure 1) are reported in Figures 4 and 5, respectively, and show broad ranges around averaged values $\theta_1 \sim \theta_2 \sim 135°$.

The orientation of a hydrogen with respect to the n and π electrons of the carbonyl group[3k] may be described through the Φ_1 parameter: 37% of the Φ_1 values are included in the ranges 0–20° and 160–180° (n electrons) and 26% in the range 70–110° (π electrons).

If we exclude the 18 carbonyl groups already involved in push–pull oxygen–carbon interactions, 4 supplementary carbonyl groups suffer 2 other kinds of push–pull interactions: 3 C=O···C=O···H–C; 1 >O···C=O···H–C. Limiting the balance to the first nine compounds of the series, those that crystallize in the $P2_12_12_1$ space group, all the carbonyl groups, except one of **3** and the two of **6**, are involved in push–pull interactions. In contrast with this observation, only seven carbonyl groups involved in push–pull interactions are registered for the second half of the series (**10–18**), the anhydrides that crystallize in achiral space groups. There is an obvious relationship between these push–pull interactions and the packing mode. The lack of any nucleophile–electrophile interaction in **6** surely results from the large pure hydrophobic surroundings protecting the anhydride group.

Pyramidalization of the Anhydride Carbonyl Groups. For each carbonyl group, we have calculated the pyramid height Δ (Figure 6); their values range from 0 to 2.3×10^{-2} Å and are reported in Table XII (supplementary material).

A total of 21 carbonyl groups have Δ values $\geq 0.5 \times 10^{-2}$ Å, i.e., significant values with respect to the standard deviations. Of these, 11 (**1–5**, **9**, **12**, **14**) are involved in O···C=O interactions, and in each case except one (a carbonyl group of **9**),[9] the oxygen nucleophile is in the same half-space (Figure 6) of the carbonyl carbon that corresponds

(6) Compounds **1–9** crystallize in the chiral $P2_12_12_1$ space group; the others crystallize in the $P2_1/n$ (**10**), $Pca2_1$ (**11**), *Pnma* (**12**), $P2_1/c$ (**13**, **14**, and **18**), *Pn* (**15**), *Pbca* (**16**), and $Pna2_1$ (**17**) achiral space groups.

(7) (a) Handal, J.; White, J. G.; Franck, R. W.; Yuh, Y. H.; Allinger, N. L. *J. Am. Chem. Soc.* **1977**, *99*, 3345–3349. (b) Mirsky, K. *Acta Crystallogr., Sect. A: Cryst. Phys. Diffr. Theor. Gen. Crystallogr.* **1976**, *A32*, 199–207.

(8) The actual symmetry of **6** may be different than the a priori C_{2v} owing to torsion around the central bond (19.6° in the crystal) induced by the nonbonded interaction between the H(9A) and H(10A) hydrogen atoms of the two methano bridges. Therefore, in solution, **6** may have two enantiomeric conformers, which allows its crystallization as a conglomerate.

(9) The O···C=O interaction is weak (d = 3.48 Å), and two C=O···H interactions (d = 2.47 and 2.52 Å) act in the half-space opposite the nucleophilic oxygen atom.

to a normal situation. As 10 of these 11 carbonyl groups are involved in Nu···C=O···El push–pull interactions, the O···El interactions do not change the Δ sign, except for **9**.[9] Another 6 carbonyl groups of this class of 21 are only involved in C=O···El interactions, El being H in 5 cases and C in 1 case; all 6 carbonyl groups belong to compounds (**10, 11, 13, 15**) that crystallize in achiral space groups. The influence of the C=O···El on the Δ sign is not obvious, as El is distributed in the two half-spaces and at close proximity to the carbonyl plane ($\Phi_1 \sim 0°$ or 180°). The last four carbonyl groups belong to compounds (**6** and **16**) without any weak electrophilic hydrogen atom, as we define it in the introduction, but this limitation may be questionable.[5a]

Among the 16 carbonyl groups that are weakly pyramidalized ($\Delta < 0.5 \times 10^{-2}$ Å), we may distinguished 7 that are involved in 2 counteracting O···C=O interactions, the oxygen nucleophiles of which are located in different half-spaces (Figure 6) with cancellation of their effect on pyramidalization. Another 6 carbonyl groups are involved in only 1 O···C=O interaction and in several C=O···El interactions; in each case except 1, 1 or 2 of the electrophiles is a carbon atom. For the last three carbonyl groups, there are no O···C=O interactions.

Whereas the role played by Nu···C=O···El interactions in the crystallization process is obvious, the influence of the C=O···El interactions on pyramidalization must be studied thoroughly. It is the subject of the MNDO calculations.

Anhydride Ring Conformations. For each anhydride cycle (five-membered ring) except **9** and **18**, the carbonyl groups ($C_\beta O_\gamma$) are out of the reference plane defined by the middle oxygen (O_δ) and the two carbon atoms (C_α and $C_{\alpha'}$) bonded to the carbonyl carbons (C_β and $C_{\beta'}$). The distances d between this plane and the carbonyl atoms have been calculated and reported in Table XIV (supplementary material). For all the molecules except two (**6** and **9**), the atoms of each carbonyl group are located in the same half-space delimited by the reference plane, and it may be observed that $|d(O_\gamma)| > |d(C_\beta)|$. Owing to the relative position of the two carbonyl groups of a molecule that may be in the same half-space or in opposite ones, the anhydride rings adopt envelope (**12, 13, 15, 16, 18A,B**) or half-chair conformations (**1–3, 4A,B, 5, 7, 8, 10, 11, 14, 17**). All the molecules crystallizing in the $P_{2_12_12_1}$ chiral group, except **6** and **9**, have a half-chair conformation that shifts the molecular symmetry from C_s to C_1 or C_{2v} to C_2. In spite of similar features, four molecules (**10, 11, 14, 17**) crystallize in achiral groups, just as the six molecules with an envelope ring do. If the nonplanarity of the anhydride ring seems to be the norm, we are unable to implicate some intermolecular interactions in the process that orients toward an envelope or a half-chair conformation.

MNDO Calculations

In order to study the efficiency of push–pull nucleophile–electrophile interactions in inducing geometrical deformation of the carbonyl of an anhydride moiety, semiempirical calculations have been carried out using the MNDO method.[10] All the geometries were optimized at the SCF level by minimizing the energy with the Davidon–Fletcher–Powell (DFP) algorithm.[11,12] In a first step, the calculations have been performed on formaldehyde, the simplest carbonyl molecule, in order to check the efficiency of these calculations in reproducing the experimental[3b] and theoretical[3c] structural features associated with separate nucleophilic and electrophilic approaches, and then with simultaneous attack. Finally, the formic anhydride was used as a second model in order to determine the influence of the second moiety of the anhydride group.

In order to allow a possible pyramidalization of formaldehyde, nearly all the geometrical variables were optimized in each calculation; the H–C distance was held constant at 1.10 Å, with the two OCH angles remaining equal to each other throughout the study. Thus, the C_{2v} symmetry of the initial molecule changes to C_s as pyramidalization occurs, the corresponding σ plane being subsequently referred to as bisector.

Nucleophilic Approach to Formaldehyde. Various nucleophilic species have been used (Table I). Their own geometrical features have been held constant at the values computed from independant MNDO calculations of isolated molecules.[13] The Li–H axis and the H_2O and CH_2O reactant C_2 axis lay in the bisector plane of the CH_2O substrate (Figure 1). For different Nu···C distances (d_1), we report in Table I the computed values of θ_2, the nucleophile attack angle, and the value of θ_1, the angle between the reactant symmetry axis and the Nu···C axis, corresponding to minimum calculated heat of formation (ΔH_f). We have also confirmed that the optimal approach occurs when the reactant nucleophilic atom is in the bisecting plane of the substrate. Furthermore, we observe a displacement of its carbon out of the plane defined by its three bonded atoms and toward the reactant (Figure 6). The corresponding pyramidalization heights (Δ) are

Table I. Relative Orientation of Nucleophilic Reactants with Respect to CH_2O Substrate: θ_2[a] Angles for Minimum ΔH_f Values

	d_1[b]				
reactant	3.5	3.0	2.7	2.5	2.2
H^-	180	178	131	120	113
LiH[c]		131	119	115	111
H_2O[d]	116	101		98	
H_2O[e]	95 (228)	94 (219)		96 (208)	
CH_2O[e]	87 (235)	94 (219)		96 (207)	

[a] Nu···C=O angle in degrees. [b] Nu···C distance in angstroms. [c] Li–H···C = 180°. [d] θ_1 180° (Figure 1, 1.2). [e] Figures in parentheses correspond to θ_1 optimized values.

Table II. ΔH_f Values[a] and Pyramidalization Heights[b] Calculated for the $CH_2O \bullet\bullet\bullet CH_2O$ System as Functions of Φ_1[c]($\theta_1 = \theta_2 = 105°$) and θ_1[c]($\theta_2 = 105°$; $\Phi_1 = 90°$)

		d_1, Å		
		3.5	3.0	2.5
Φ^1	0	−64.9 (0.38)	−62.7 (1.14)	−54.7 (4.04)
	45	−64.9 (0.33)	−62.7 (1.08)	−54.9 (3.92)
	90	−64.8 (0.26)	−62.7 (1.03)	−55.0 (3.81)
θ_1	105	−64.8 (0.26)	−62.7 (1.03)	−55.0 (3.81)
	130	−65.5 (0.26)	−64.0 (0.83)	−57.9 (3.10)
	155	−65.9 (0.25)	−64.7 (0.78)	−59.2 (2.94)
	180	−66.2 (0.25)	−65.1 (0.77)	−59.8 (2.91)
	205	−66.4 (0.25)	−65.3 (0.78)	−60.1 (2.91)
	230	−66.4 (0.27)	−65.2 (0.81)	−59.6 (2.96)
	255	−66.1 (0.28)	−64.4 (0.89)	−57.1 (3.15)

[a] In kilocalories per mole. [b] Figure 6; second CH_2O molecule; Δ × 10^2 Å in parentheses. [c] In degrees.

(10) Dewar, M. J. S.; Thiel, W. *J. Am. Chem. Soc.* **1977**, *99*, 4899–4907, 4907–4917.
(11) (a) Davidon, W. C. *Comput. J.* **1968**, *10*, 406–410. (b) Fletcher, R. *Ibid.* **1965**, *8*, 33–41. (c) Fletcher, R.; Powell, M. J. D. *Ibid.* **1963**, *6*, 163–168.
(12) Thiel, W. *QCPE* **1982**, *14*, 438.
(13) Li–H, 1.38 Å; $H_2O(C_{2v})$ O–H, 0.943 Å; HOH, 106.8°; $CH_2O(C_{2v})$, C–H, 1.10 Å; C=O, 1.22 Å; OCH, 122°.

Table III. Pyramidalization Heights ($\Delta \times 10^2$ Å) and Optimized θ_1 Values[a,b] as Functions of Nucleophile–Electrophile Distance (d_1) and of θ_2 Angle[b] for the CH_2O Substrate

		d_1, Å		
reactant	θ_2[b]	3.5	3.0	2.5
CH_2O[c]	180	0.0 (179)	0.0 (179)	0.0 (179)
	150	0.27 (181)	1.45 (182)	4.59 (180)
	135	0.39 (180)	1.35 (191)	4.77 (188)
	120	0.29 (202)	1.11 (199)	3.95 (195)
	105	0.24 (216)	0.78 (210)	2.76 (201)
	90	0.17 (233)	0.44 (222)	1.97 (210)
H_2O[c]	105	0.27	0.82	3.07
HO^-[d]	105	0.16	0.78	3.35
H_3N[e]	105	0.26	1.05	3.95

[a] Figures in parentheses correspond to θ_1 optimized values. [b] In degrees. [c] $\Phi_1 = 90°$. [d] HO···C angles = 180°; H–O optimized in each calculation. [e] C_3 axis collinear with N···C axis; N–H fixed at 1.007 Å, as in isolated NH_3 molecule optimized in a MNDO calculation.

Table IV. ΔH_f Values[a] and Pyramidalization Heights[b] Calculated for the $CH_2O \cdots$J–K System as Functions of ψ^{14} and θ_1 Angles[c] for $d_2 = 2.5$ Å and $\theta_2 = 180°$

		ψ		
reactant, J–K	θ_1	0	45	90
H–F	90	−88.9 (0.24)	−89.0 (0.33)	−88.8 (0.00)
	105	−90.2 (0.14)	−90.4 (0.14)	−90.5 (0.00)
	120	−91.1 (0.10)	−91.2 (0.08)	−91.4 (0.00)
	150	−92.0 (0.05)	−92.1 (0.04)	−92.1 (0.00)
	180	−92.3 (0.00)		
Li–H	90	−19.0 (2.11)	−19.7 (1.50)	−20.3 (0.00)
	105	−19.3 (1.79)	−20.1 (1.24)	−20.9 (0.00)
	120	−20.1 (1.47)	−20.8 (1.02)	−21.5 (0.00)
	150	−21.8 (0.77)	−22.1 (0.52)	−22.4 (0.00)
	180	−22.5 (0.00)		

[a] In kilocalories per mole. [b] $\Delta \times 10^2$ Å in parentheses. [c] In degrees.

reported in parentheses in Table II with the associated ΔH_f values as functions of Φ_1 and θ_1 parameters for the $CH_2O \cdots CH_2O$ system. ΔH_f values decrease with distances d_1, but do not significantly change with Φ_1. On the other hand, the pyramidalizations are maximum with $\Phi_1 = 0°$ when an oxygen lone pair of the reactant is oriented toward the substrate carbon atom. Table III shows pyramidalizations being maximum in the range $\theta_2 = 135$–$150°$, but this geometrical situation corresponds to higher ΔH_f values.

For $\theta_2 = 105°$, the pyramidalization efficiency of the reactants is in the order $H_3N > HO^- \sim H_2O > CH_2O$.

Therefore, the MNDO calculations lead to general conclusions in agreement with those of previous experimental and theoretical studies.[3] These conclusions are available whatever the reactant species.

Electrophilic Approach to Formaldehyde. A total of three electrophilic species (H^+, HF, and LiH) have been used. With the electrophile H^+, the preferred approach corresponding to minimum ΔH_f values is in the plane of the CH_2O substrate ($\psi = 90°$),[14] as experimentally observed for C=O···H contact.[5c] For $d_2 = 2.5$ and 2.0 Å, the optimized θ_1 values (Figure 1, J = H^+) are 158 and 138°, respectively. With the hydrogen of HF and the lithium of LiH as electrophilic atoms (Table IV), the preferred approach (ΔH_f minimum) occurs for $\theta_2 = 180°$.

The MNDO calculations show that the electrophilic approach takes place toward the substrate oxygen atom, and as in the nucleophilic approach, *a pyramidalization appears* (except for $\theta_2 = 180°$ or $\psi = 90°$) *with the substrate carbon atom moving in the half-space where the electrophile reactant is located.* The pyramidalization efficiencies may be classified as Li–H > $BH_3 \sim CH_2O$ > HF (Table V).

(14) ψ corresponds to the dihedral angle between the HCH bisector and C=O···El planes.

Table V. Pyramidalization Heights ($\Delta \times 10^2$ Å) as a Function of Nucleophile–Electrophile Distance (d_2) to CH_2O Substrate for $\theta_1 = 105°$ and $\psi^{14} = 0°$

	d_2, Å		
electrophilic reactant	3.5	3.0	2.5
HF[a]	0.05	0.07	0.13
LiH[a]	0.46	0.94	1.83
CH_2O[a,b]	0.07	0.15	0.39
BH_3[c]	0.07	0.17	0.53

[a] $\theta_2 = 105°$; $\Phi_2 = 180°$. [b] $\Phi_3 = 90°$. [c] CH_2O oxygen atom on BH_3, C_3 axis; BH_3 symmetry allowed to change from D_{3h} to C_{3v}; B–H fixed at 1.155 Å from the MNDO calculation of the isolated molecule.

Table VI. Pyramidalization Heights ($\Delta \times 10^2$ Å) for the $H_2O \cdots CH_2O \cdots$LiH System[a] ($\Delta_{add} \times 10^2$ Å Values[b] in Parentheses)

$CH_2O \cdots$ LiH		d_1, Å		
geometry	variable	3.5	3.0	2.5
	d_2			
I[c]	3.0 Å	−0.75 (−0.67)	−0.01 (−0.12)	2.21 (2.13)
	2.5 Å	−1.64 (−1.56)	−0.92 (−1.01)	1.42 (1.24)
	θ_2			
II[d]	(360–105)°	1.90 (2.10)	2.43 (2.65)	4.69 (4.90)
	(360–120)°	1.58 (1.74)	2.18 (2.29)	4.16 (4.54)
	(360–150)°	0.96 (1.04)	1.79 (1.59)	3.75 (3.84)
	d_2			
III[e,g]	3.0 Å	0.21 (0.27)	0.81 (0.82)	3.04 (3.07)
	2.5 Å	0.18 (0.27)	0.79 (0.82)	3.04 (3.07)
	d_2			
IV[f,g]	3.0 Å	0.32 (0.27)	0.93 (0.82)	3.04 (3.07)
	2.5 Å	0.17 (0.27)	0.80 (0.82)	3.04 (3.07)

[a] $H_2O \cdots CH_2O$ parameters (Figure 1, 1.2): $\theta_1 = \theta_2 = 105°$; $\Phi_1 = \Phi_3 = 90°$; Φ_2 180°. [b] $\Delta_{add} = \Delta(H_2O \cdots CH_2O) + \Delta(CH_2O \cdots LiH)$; $\Delta(H_2O \cdots CH_2O)$ values from Table III; $\Delta(CH_2 \cdots LiH)$ values from Table V. [c] $CH_2O \cdots LiH$ parameters (Figure 1, 1.3): $\theta_1 = \theta_2 = 105°$; $\psi = 0°$; $\Phi_2 = 180°$. [d] Parameters: $d_2 = 2.5$ Å; $\theta_1 = 105°$; $\psi = 0°$ $\Phi_2 = 180°$. [e] Parameters: $\theta_1 = \theta_2 = 105°$; $\psi = 90°$; $\Phi_2 = 180°$. [f] Parameters: $\theta_1 = \theta_2 = 180°$. [g] $\Delta_{add} = \Delta(H_2O \cdots CH_2O)$.

Push–Pull Nucleophile–Electrophile Approach to Formaldehyde. Pyramidalization height is defined either positive or negative, depending on whether the substrate carbon is moving toward the nucleophilic reactant (in the same half-space) or away from it (in the opposite half-space).

Since the H_2O molecule (as nucleophile) and the LiH molecule (as electrophile) provide significant and comparable pyramidalization when they separately interact with CH_2O substrate, the calculations were performed on the $H_2O \cdots CH_2O \cdots$LiH system for different geometries (Table VI), which locate the reactants in opposite half-spaces (I as in Figure 6) or in the same half-space (II) or with the LiH molecule in the plane of the substrate molecule (III and IV). The additivity of separate pyramidalizations $\Delta_{add} = \Delta(H_2O \cdots CH_2O) + \Delta(CH_2O \cdots LiH)$ (values in parentheses in Table VI, geometries I and II) is a satisfactory hypothesis, accounting for the counteraction of the two reactants on pyramidalization when they are in opposite half-spaces (geometry I in Table VI) and for an increased pyramidalization when they are in the same half-space (geometry II). If the electrophile reactant is in the plane of the substrate molecule (geometries III and IV), its presence does not change the pyramidalization induced by the nucleophile reactant very much.

Table VII. Pyramidalization Heights ($\Delta \times 10^2$ Å) for HC(O)OC(O)H Involved in Different Interactions ($\Delta_{add} \times 10^2$ Å[a] Values in Parentheses)

systems	d,[b] Å 3.5	3.0	2.5
H_2O···CHO(O–CHO)[c,d]	0.37	1.44	4.82
(CHO–O)CHO···CH_2O[d,e]	0.00	0.08	0.59
(CHO–O)CHO··LiH[f]	0.85	1.71	3.03
H_2O···CHO(O–CHO)··· CH_2O[g]	−0.07 (−0.22)	0.84 (0.85)	4.22 (4.23)
H_2O···CHO(O–CHO)···LiH[h]	−0.50 (−0.48)	0.53 (0.59)	4.04 (3.97)

[a] $\Delta_{add} = \Delta[H_2O\cdots CHO(O–CHO)] + \Delta[(CHO–O)CHO\cdots El]$. [b] $d = d_1$ for H_2O···CHO(O–CHO) and H_2O···CHO(O–CHO)···El; $d = d_2$ for (CHO–O)CHO···El. [c] $\theta_1 = \theta_2 = 105°$; $\Phi_1 = \Phi_3 = 90°$; $\Phi_2 = 180°$. [d] Figure 1, 1.2. [e] Cf. Figure 1, 1.1. [f] $\theta_1 = 105°$; $\theta_2 = 180°$; $\Phi_1 = 90°$; cf. Figure 1, 1.3. [g] $d_2 = 2.5$ Å; cf. footnotes *b*, *c*, and *d*. [h] $d_2 = 3.5$ Å; cf. footnotes *b*, *c*, and *e*.

Similar results have been obtained with H_2O···CH_2O···HF and CH_2O···CH_2O···CH_2O systems. For the last one, see Table XIII (supplementary material).

Nucleophile and Electrophile Approaches to Formic Anhydride. In order to check the availability of a transfer of the formaldehyde results to anhydrides, some calculations have been performed with formic anhydride HC(O)OC(O)H as substrate in its *s-E,s-E* conformation (C_{2v} symmetry).[15] In the course of the reactant attack on one of the carbonyl groups (C_a=O_a), all the parameters were fixed to initial values[15] except for C_aO_a and C_aO distances and $O_aC_aH_a$ and O_aC_aO angles. As a result of the intermolecular interactions, the system is no longer planar, and a pyramidalization arises at the C_a level. Owing to the asymmetry of the substrate molecule, the bisector is now defined as the plane bisecting the dihedral angle between the $O_aC_aH_a$ and O_aC_aO planes, the latter containing the remaining atoms of the molecule.

Simple and push–pull interactions are investigated in Table VII; as for CH_2O substrate, we observe good agreements for the so-called additivity rule about the push–pull pyramidalizations.

Nonplanar Anhydride Conformations. Owing to the experimental results suggesting that intramolecular interactions, such as oxygen orbital overlap, prevent the anhydride cycle from flattening, we calculate the envelope and half-chair conformation energies of *s-E* formic anhydride for different values of the $HO_\delta H/HO_\gamma O_\delta$ by steps of 0.5°, the hydrogen atoms and middle O_δ atom kept fixed as in the fully relaxed planar molecule. Calculations performed with only the hydrogen atoms kept fixed give similar results. The conformation at the energy minimum is very close to the planar one, the dihedral angle Φ and the energy difference ΔH deviating from 2° and 5 cal·mol^{-1} at the most, respectively. But the potential energy surfaces appear to be very flat around the energy minimum; for $\Delta\Phi = 10°$, $\Delta H = 15$ and 330 cal·mol^{-1} for half-chair and envelope conformations, respectively.

Therefore, deviations from the planar conformation look very easy and may be governed by the balance of soft intermolecular interactions, even pure Van der Waals ones. The evolution toward the envelope or the half-chair conformation appears to be easier in the latter case, which corresponds to 12 observations versus 6 for the envelope. Moreover, as the anhydride ring is puckered, a carbonyl group pyramidalization occurs; for $\Delta\Phi = 10°$, $\Delta = 0.4$ and 1.3×10^{-2} Å for half-chair and envelope conformations, respectively.

(15) Initial geometrical parameters obtained by MNDO calculations: C=O, 1.2185 Å; C–O, 1.3722 Å; H–C=O, 126.0°; O–C=O, 116°; C–O–C, 123.9°; H–C fixed at 1.10 Å.

Discussion

In agreement with earlier conclusions from ab initio calculations,[3c,e] whatever the nucleophilic reagent (>O or C=O), its optimal approach occurs toward the C=O carbon atom, in the bisector ($\Phi_3 \sim 90°$) with θ_2 angles (Figure 1, 1.1 and 1.2) generally greater than 90°, and in the range 100–110° as the O···C distance decreases (Tables VIII and IX, Figure 7; supplementary material). The MNDO calculations are in good agreement with the experimental results (Table I). Moreover, it is noticeable that θ_1 and θ_2 values (Table I) and pyramidalization heights (Table III) corresponding to H_2O and CH_2O as nucleophilic reagents are, respectively, close together. Therefore, these calculations a posteriori justify our decision to consider both C=O···C=O and >O···C=O interactions (Figures 2 and 3). Results from H_2O···CH_2O interactions (Table I) show variations of θ_2 when θ_1 varies from a 180° fixed value to the optimized values (~220°); in anhydride crystals, θ_2 does not depend on θ_1, which range from 115 to 165° and from 230 and 255° ($360 - \theta_1$ when $\Phi_2 < 90°$) for θ_2 values ranging from 100 to 120° (Figure 8, supplementary material). It is clear that less than half the O···C=O interactions correspond to optimal θ_1 values (>180°; see Table II); the packing appears to be mainly on the θ_2 control.

The electrophilic approach preferentially occurs in the plane of the CH_2O molecule with H^+ as electrophile and in the prolongation of the carbon–oxygen double bond with HF and LiH (Table IV). For each θ_1 value, the calculated energy differences corresponding to $\psi = 0°$ and $\psi = 90°$ do not exceed 0.4 (HF) or 1.7 kcal·mol^{-1} (LiH). This can be correlated with anhydride crystal data, which show an almost random dispersion of θ_1 values (similar to ψ) for C=O···H–C, C=O···C–O, and C=O···C=O interactions[16] (Tables X, XI, and VIII, respectively; supplementary material).

In contrast to the nucleophilic approach, which is very dependent on geometry and consequently on steric hindrance control, the electrophilic approach is efficient whatever its orientation, therefore quite independent of steric factors. This first conclusion may be an useful statement for structure–reactivity correlations.

Turning now to the carbonyl group pyramidalization, which may be qualitatively related to the transition-state geometry (reactantlike or productlike), the MNDO calculations obviously confirm that as long as a nucleophilic or an electrophilic approach occurs in the plane of the CH_2O molecule, no pyramidalization is observed. But, as soon as the reactant deviates from this plane, a pyramidalization arises, the CH_2O carbon moving toward the reactant (Tables III and IV). In the anhydride crystals, we have not observed any case with θ_2(Nu···C=O) or θ_1(C=O···El) values equal to 180°.

The MNDO calculations lead to some supplementary remarks:

(1) In the course of the reactant approach, Δ is primarily dependent on the d_1 or d_2 distance; subsequent calculations show that the H^-···CH_2O system continuously tends toward the formation of the CH_3O^- anion, with maximum pyramidalization when H^- is located at distances in the range 2.5–1.2 Å.

(2) The pyramidalizations due to HO^- and H_2O reactants are close together (Table III), which suggest that no electrostatic effect is involved.

(3) According to the previous hypothesis related to crystal structure analysis,[3b,f] nitrogen atom is more nucleophilic than oxygen, if judged by Δ values (Table III).

(16) Cossu, M. Thèse Doctorat ès sciences physiques, Université de Provence, Marseille, 1983.

(4) At a given distance, the pyramidalizations induced by nucleophiles are generally greater than those induced by electrophiles.

(5) Larger Δ values are obtained with LiH as electrophile, which reveals a stronger interaction, even at long distances (Table V); indeed, the more diffuse lithium orbitals allow a larger overlap with the CH_2O orbitals.

(6) The pyramidalizations look almost insensitive to the reactant (nucleophile or electrophile) orientation, providing the nucleophilic or electrophilic atom is well located.

The MNDO-calculated Δ values related to the nucleophilic approach are roughly 0.3×10^{-2} Å at $d_1 = 3.5$ Å, 0.80×10^{-2} Å at $d_1 = 3.0$ Å, and 3×10^{-2} Å at d_1 2.5 Å, in qualitative agreement with the values observed from the anhydride crystals (Δ up to 2.3×10^{-2} Å with d_1 and d_2 distances in the range 2.9–3.6 Å). However, in a number of cases, the experimental values are smaller and occasionally close to zero (Table XII, supplementary material). Our push–pull hypothesis has been well supported by the MNDO calculations (Tables VI and VII), which predict an additivity rule for Δ with possible cancellation or inverse pyramidalizations (with respect only to those induced by the nucleophile reactant) when the nucleophilic and electrophilic reactants are located in opposite half-spaces of the carbonyl group (Table VI, geometry I).

Indeed, Table VI shows that the differences between Δ_{add} and computed Δ values do not exceed 0.2×10^{-2} Å. The deviations are maximum for geometry II, because the H_2O oxygen and the lithium atoms are close together (O···Li = 2 Å for $d_1 = d_2 = 2.5$ Å) and consequently can interact. When LiH moves from one half-space (geometry I) to the other (geometry II), the reactant net charges, negative on LiH and positive on H_2O, vary by –0.079e and +0.086e, respectively, indicating an electronic transfer from H_2O to LiH.

In order to check whether this additivity rule is operational upon other reactants, further calculations were carried out on H_2O···CH_2O···HF and CH_2O···CH_2O···CH_2O push–pull systems (Table XIII, supplementary material). In both cases, the results show that Δ and Δ_{add} values are still close together. It may be expected that the so-called additivity rule is fairly general. Moreover, in some cases, namely when there are no significant interactions between reactants, one would reasonably expect that this rule could still apply with more than two nucleophile–electrophile interactions on the carbonyl group, which is very frequent in the crystals (Table XII, supplementary material).

Finally, in order to extend the previous conclusions from CH_2O as substrate to anhydride moieties, further calculations were devoted to the HC(O)OC(O)H system and focused on pyramidalizations (Table VII). For similar geometries, the Δ values determined for this anhydride are larger than the CH_2O values by an average factor of about 1.6. This increase is larger than the one predicted on the simple change in bond lengths[17] owing to the pyramidal basis extension. Therefore, such an observation suggests that both nucleophilic and electrophilic approaches are more efficient on anhydrides than on simple carbonyl compounds.

In spite of calculations and experimental data corresponding to early stages of addition reaction paths, these pyramidalization comparisons suggest productlike and reactantlike transition states, respectively, for anhydrides and simple carbonyl compounds.

Once again, the additivity rule is operational (Table VI), which suggests returning to the anhydride crystal data from which some typical examples may be extracted. Subsequently, the efficiency or the weakness of the different interactions will be qualitatively determined from the analysis of different geometrical data,[16] in particular the intermolecular distances d, but also θ_2 (Table III), Φ_3, θ_1 and Φ_1. Some of the highest observed pyramidalization heights ($\Delta > 1.5 \times 10^{-2}$ Å) correspond either to efficient O···C=O interactions[18] (with[18a] or without[18b] weak C=O···El interactions) or to efficiency of both located in the same half-space.[19] Another case[20] corresponding to a nucleophilic oxygen and two electrophilic carbons, located in the same half-space, shows a weaker pyramidalization ($\Delta = 0.5 \times 10^{-2}$ Å), but their effect is surely counteracted by an electrophilic hydrogen located in the other half-space at short intermolecular distance (2.36 Å) from the carbonyl oxygen atom. Weak pyramidalizations ($\Delta < 0.5 \times 10^{-2}$ Å) are observed either for efficient interactions, but with reactants in opposite half-spaces[21] or for Nu···C=O and C=O···El interactions, both being too weak.[22]

Disagreements[23] between experimental data and the model are observed; four of these seven carbonyl groups show significant pyramidalizations ($\Delta \geq 0.5 \times 10^{-2}$ Å) without any efficient interactions. Similar cases are observed for carbonyl groups not involved in O···C=O interactions[24] or in any nucleophile–electrophile interactions.[25] As these carbonyl groups belong to puckered anhydride rings (Table XIV, supplementary material), the MNDO calculations have shown that pyramidalizations may occur without any nucleophile–electrophile interaction. Therefore, it only remains to understand the origin of the puckering of these molecules; soft packing interactions may be involved, but their analysis is not possible at the present time.

Acknowledgment. We acknowledge the Office Central de Mécanographie d'Abidjan, where the calculations have been performed on IBM 4341 computers.

Registry No. 1, 2746-19-2; 2, 6118-51-0; 3, 129-64-6; 4, 56587-27-0; 5, 36843-54-6; 6, 73679-38-6; 7, 108-31-6; 8, 108-30-5; 9, 81-84-5; 10, 75813-98-8; 11, 56587-28-1; 12, 56-25-7; 13, 24327-08-0; 14, 51447-09-7; 15, 73711-63-4; 16, 73654-75-8; 17, 85-44-9; 18, 4480-83-5; HCHO, 50-00-0; H^-, 12184-88-2; LiH, 7580-67-8; H_2O, 7732-18-5.

Supplementary Material Available: Listings of experimental geometrical parameters (Tables VIII–XI), calculated pyramidalization heights (Tables XII and XIII), and conformations of the anhydride rings (Table XIV) and Figure 7 of θ_2 as a function of d_1 (8 pages). Ordering information is given on any current masthead page.

(17) The increase related to this lengthening is $\lambda \sim 1 + [(C–O) - (C–H)/3(C–H)] \sim 1.08$ with $\Delta(C–O) = \lambda\Delta(C–H)$.

(18) (a) 4: C(8B) = O(2B); Nu, O(3B); El, H(1A), H(5B). (b) 3: C(9) = O(3); Nu, O(2).

(19) 1: C(9) = O(3); Nu, O(2); El, H(3). 4: C(9B) = O(3B); Nu, O(3B); El, C(9B), C(8B).

(20) 3: C(8) = O(2); Nu, O(2); El, C(9), C(8), H(3).

(21) 7: C(5) = O(7); Nu, O(6); El, C(2), H(8); C(2) = O(6); Nu, O(6), O(7); El, C(5), C(2); H(8). 8: C(4) = O(7); Nu, O(6), O(7); El, C(1), C(4), H(11); C(1) = O(6); Nu, O(7), O(6); El, C(4), C(1).

(22) 2: C(9) = O(3); Nu, O(1); El, C(8), H(4). 5: C(15) = O(4); Nu, O(2); El, C(11), C(14), H(10). 7: C(7) = O(7); Nu = O(8); El = H(4).

(23) 1: C(8) = O(2); $\Delta = 1.7 \times 10^{-2}$ Å; Nu, O(2); El, C(9) (weak interactions). 2: C(8) = O(2); $\Delta = 0.1 \times 10^{-2}$ Å; one strong interaction (H(4)). 5: C(14) = O(3); $\Delta = 0.8 \times 10^{-2}$ Å; Nu, O(4); El, C(12), H(9) (weak interactions). 9: C(11) = O(2); $\Delta = 2.3 \times 10^{-2}$ Å; Nu, O(2); El, C(11), H(2) (weak interactions); C(12) = O(3); $\Delta = 1.1 \times 10^{-2}$ Å; one strong interaction (H(7)), but inverse pyramidalization. 12: C(4) = O(3); $\Delta = 1.5 \times 10^{-2}$ Å; Nu, O(1); El, C(2) (weak interactions). 17: C(8) = O(8); $\Delta = 0.2 \times 10^{-2}$ Å; Nu, O(8) (strong interaction); El, C(7), C(8), H(3) (all the reactants being in the same space).

(24) 10: C(13) = O(16); $\Delta = 1.0 \times 10^{-2}$ Å; C(14) = O(17); $\Delta = 0.8 \times 10^{-2}$ Å. 11: C(8) = O(2); $\Delta = 0.5 \times 10^{-2}$ Å; C(9) = O(3); $\Delta = 0.7 \times 10^{-2}$ Å. 13: C(10) = O(3); $\Delta = 0.7 \times 10^{-2}$ Å. 15: C(11) = O(14); $\Delta = 1.0 \times 10^{-2}$ Å; C(12) = O(15); $\Delta = 1.4 \times 10^{-2}$ Å.

(25) 6: C(11) = O(14); $\Delta = 0.9 \times 10^{-2}$ Å. 16: C(11) = O(14); $\Delta = 0.9 \times 10^{-2}$ Å; C(12) = O(15); $\Delta = 1.3 \times 10^{-2}$ Å.